Cell PRESS
Cancer Cell
Article

An Activated ErbB3/NRG1 Autocrine Loop Supports In Vivo Proliferation in Ovarian Cancer Cells

Qing Sheng,[1,3] Xinggang Liu,[1,3] Eleanor Fleming,[1,3] Karen Yuan,[1,3] Huiying Piao,[2,3,4] Jinyun Chen,[6] Zeinab Moustafa,[6] Roman K. Thomas,[7,8,9] Heidi Greulich,[2,3,5,10] Anna Schinzel,[2,3,10] Sara Zaghlul,[1,3] David Batt,[6] Seth Ettenberg,[6] Matthew Meyerson,[2,3,10] Birgit Schoeberl,[11] Andrew L. Kung,[3,12] William C. Hahn,[2,3,10] Ronny Drapkin,[2,3,4] David M. Livingston,[1,3,*] and Joyce F. Liu[1,2,3]

[1]Department of Cancer Biology
[2]Department of Medical Oncology
Dana-Farber Cancer Institute, Boston, MA 02115, USA
[3]Harvard Medical School, Boston, MA 02115, USA
[4]Department of Pathology
[5]Department of Medicine
Brigham and Women's Hospital, Boston, MA 02115, USA
[6]Novartis Oncology, Cambridge, MA 02139, USA
[7]Max Planck Institute for Neurological Research with Klaus-Joachim Zülch Laboratories, Max Planck Society and the Medical Faculty of the University of Köln, D-50931 Köln, Germany
[8]Department I of Internal Medicine and Center of Integrated Oncology, University of Köln, D-50937 Köln, Germany
[9]Chemical Genomics Center of the Max Planck Society, D-44227 Dortmund, Germany
[10]Broad Institute of Harvard University and the Massachusetts Institute of Technology, Cambridge, MA 02142, USA
[11]Merrimack Pharmaceuticals, Cambridge, MA 02139, USA
[12]Department of Pediatric Oncology, Dana-Farber Cancer Institute and Children's Hospital, Boston, MA 02115, USA
*Correspondence: david_livingston@dfci.harvard.edu
DOI 10.1016/j.ccr.2009.12.047

SUMMARY

Ovarian cancer is a leading cause of death from gynecologic malignancies. Treatment for advanced-stage disease remains limited and, to date, targeted therapies have been incompletely explored. By systematically suppressing each human tyrosine kinase in ovarian cancer cell lines by RNAi, we found that an autocrine signal-transducing loop involving NRG1 and activated ErbB3 operates in a subset of primary ovarian cancers and ovarian cancer cell lines. Perturbation of this circuit with ErbB3-directed RNAi decreased cell growth in three-dimensional culture and resulted in decreased disease progression and prolonged survival in a xenograft mouse model of ovarian cancer. Furthermore, a monoclonal ErbB3-directed antibody (MM-121) also significantly inhibited tumor growth in vivo. These findings identify ErbB3 as a potential therapeutic target in ovarian cancer.

INTRODUCTION

Some tumors are dependent upon the continuous activity of a single oncogene for their proliferation and survival despite their having accumulated other genetic and epigenetic changes (Sharma and Settleman, 2007; Weinstein, 2002; Weinstein and Joe, 2006, 2008). Although only a few such "addicting" oncogenes have been identified, the development of drugs that antagonize the functions of some of their products has significantly changed the field of cancer treatment. Such "targeted" therapies offer potential advantages, including a reduction in nonspecific drug-associated toxicity. Furthermore, the identification of patient populations whose tumors are addicted to an oncogene of interest has made possible the first steps toward

Significance

In this report is described a distinct role for an NRG1-driven/activated-ErbB3 autocrine loop in promoting cell proliferation in human ovarian cancer cells. In a murine xenograft model, treatment with either an inducible ErbB3-directed RNAi or an ErbB3-directed monoclonal antibody resulted in significantly decreased tumor growth. Moreover, the NRG1-driven/activated-ErbB3 phenotype is present in a significant fraction of primary advanced-stage human ovarian cancers. Taken together, these results strongly suggest that ErbB3 and/or NRG1 have the potential to serve as rational treatment targets in advanced-stage ovarian cancer.

clinical application of mechanism-based therapies in appropriate patients. Of particular interest in targeted cancer therapy research are the tyrosine kinases. Some of these enzymes are central regulators of cell signaling pathways that control a variety of cellular homeostatic processes that, when corrupted, trigger abnormal cell proliferation, disorderly differentiation, enhanced survival and motility, and/or invasion by relevant tumor cells (Hunter, 1998; Mustelin and Hunter, 2002). In some human tumors, certain tyrosine kinases have become hyperactivated through mutation, and their activation can lead to a state of oncogene dependence (Blume-Jensen and Hunter, 2001; Sharma and Settleman, 2007). Drugs that inhibit oncogenic tyrosine kinases, such as imatinib, erlotinib, and trastuzumab, have become effective cancer therapies, further underlining the importance of these enzymes as valuable drug targets (Mustelin and Hunter, 2002).

Ovarian cancer is the leading cause of death from gynecologic malignancy in the United States, with an estimated 21,550 cases and 14,600 deaths occurring in 2009 (Jemal et al., 2009). Surgery and platinum-based chemotherapy remain the standard of care for initial treatment. Although initial response rates are high, the disease recurs in a large majority of patients and becomes increasingly platinum resistant (Modesitt and Jazaeri, 2007). In a setting of platinum-resistant ovarian cancer, response rates to subsequent chemotherapy are low, and death regularly ensues. Thus, new therapeutic approaches are needed.

The identification of potential addicting oncogene targets remains incompletely explored in ovarian cancer. Multiple protein tyrosine kinases, including EGFR, Her-2, ErbB3, PDGFR, and EphA2, have been found to be overexpressed in malignant ovarian tumors by comparison with normal ovarian tissue (Apte et al., 2004; Henriksen et al., 1993; Psyrri et al., 2005; Seiden et al., 2007; Shepard et al., 1991; Tanner et al., 2006; Thaker et al., 2004). However, it remains unclear what roles these tyrosine kinases play in tumor development and survival. Indeed, to date, no specific addicting target oncoprotein has been identified and validated in ovarian cancer.

RNA interference (RNAi) represents a powerful tool that can be used in a comprehensive manner to search for genes that, when depleted, trigger cell death or proliferation arrest in tumor cells. In this study, we searched for such genes in ovarian cancer cell lines using a previously described, lentivirally delivered short-hairpin RNA (shRNA) library targeting tyrosine kinases (Moffat et al., 2006). In addition, we explored the mechanism by which the product of the tyrosine kinase gene that emerged as the leading validated hit in the screen supports ovarian cancer cell survival or proliferation. We also investigated whether the same gene product is active in primary ovarian cancer cells.

RESULTS

ErbB3 Supports Ovarian Cancer Cell Proliferation

Members of a library consisting of 387 lentiviruses, each harboring a unique shRNA targeting one of 80 human tyrosine kinases, were introduced individually into SKOV3 ovarian cancer cells (see Table S1 available online). shRNAs targeting 6 of the 80 kinases screened scored positively (Table S1, highlighted rows; see Supplemental Experimental Procedures for criteria of positive hits). Sixty-two shRNAs directed at these kinases as well as at kinases that were hit only once in the SKOV3 screen were selected for a secondary screen performed in OVCAR8 cells, another ovarian cancer cell line. In this screen, EphA4, ErbB3, and KDR again scored positively, with ErbB3 scoring as the strongest hit in both ovarian cancer cell lines (Figure 1A). Validation studies were performed by transfecting OVCAR8 cells with four nonoverlapping ErbB3-directed small interfering RNAs (siRNAs), each of which also induced cell toxicity as measured by an ATP-based CellTiter-Glo assay, consistent with the results of the initial screens (Figure 1B). All of these siRNA sequences efficiently reduced endogenous ErbB3 protein expression to near-background levels (Figure 1B) and significantly decreased surface ErbB3 levels as revealed by FACS analysis (data not shown). No evidence of significant cell death was observed by FACS analysis or Annexin-V staining following siErbB3 transduction, suggesting that the observed effects in OVCAR8 cells are secondary to inhibition of cell proliferation (data not shown).

To further test whether the antiproliferative effect of ErbB3 RNAi on OVCAR8 cells was specific to ErbB3 loss, we created an ErbB3 cDNA species that was resistant to the designated siRNA through the introduction of "silent" base-pair mutations at the siRNA recognition site. Introduction of this siRNA-immune ErbB3 cDNA into OVCAR8 cells significantly increased the ErbB3 protein level, and this high level persisted even in the presence of siErbB3 (Figure 1C). The total level of activated ErbB3, however, was not elevated much above that detected in naive OVCAR8, suggesting that activation of ErbB3 is tightly regulated. siErbB3 did reduce T308 AKT phosphorylation in OVCAR8 cells transduced with vector alone as compared with control siRNAs (Figure 1C). In the absence of exogenously added NRG1, the ectopically overexpressed ErbB3 failed to rescue the defect in cell proliferation, despite a partial restoration of both Y1289 phosphorylation of ErbB3 and T308 phosphorylation of AKT (Figures 1C and 1D). However, significant biochemical and biological reversal of the effect of the siRNA was achieved when NRG1 was added to cells containing the ectopically overexpressed, siRNA-immune version of ErbB3 (Figures 1C and 1D). This requirement for coexpression of ligand to achieve significant rescue may reflect an absolute need for ligand and otherwise insufficient endogenous ligand production by OVCAR8 cells in this experimental setting. Moreover, because five nonoverlapping ErbB3 shRNAs and four ErbB3 siRNAs demonstrated a similar growth inhibition phenotype (Figure S1), and exogenously expressed siRNA-immune ErbB3 cDNA restored cell growth in the presence of NRG1, we conclude that selective loss of ErbB3 function can inhibit the proliferation of certain cultured ovarian cancer cells.

Comparison of the Effects of ErbB3 Depletion on Ovarian Cancer Cell Lines with Different ErbB3 Activation Status

Given the observations with SKOV3 and OVCAR8 cells, a collection of ovarian cancer cell lines was surveyed for their ErbB3 status (Figure 2A; EGFR and Her-2 status were also surveyed; see Figure S2). Of 16 cell lines examined, ErbB3 was expressed and constitutively activated in 9 and present but not activated in 6. One cell line (HeyA8) did not express ErbB3. Activation of ErbB3 was indicated by phosphorylation of Y1289 (Kim et al.,

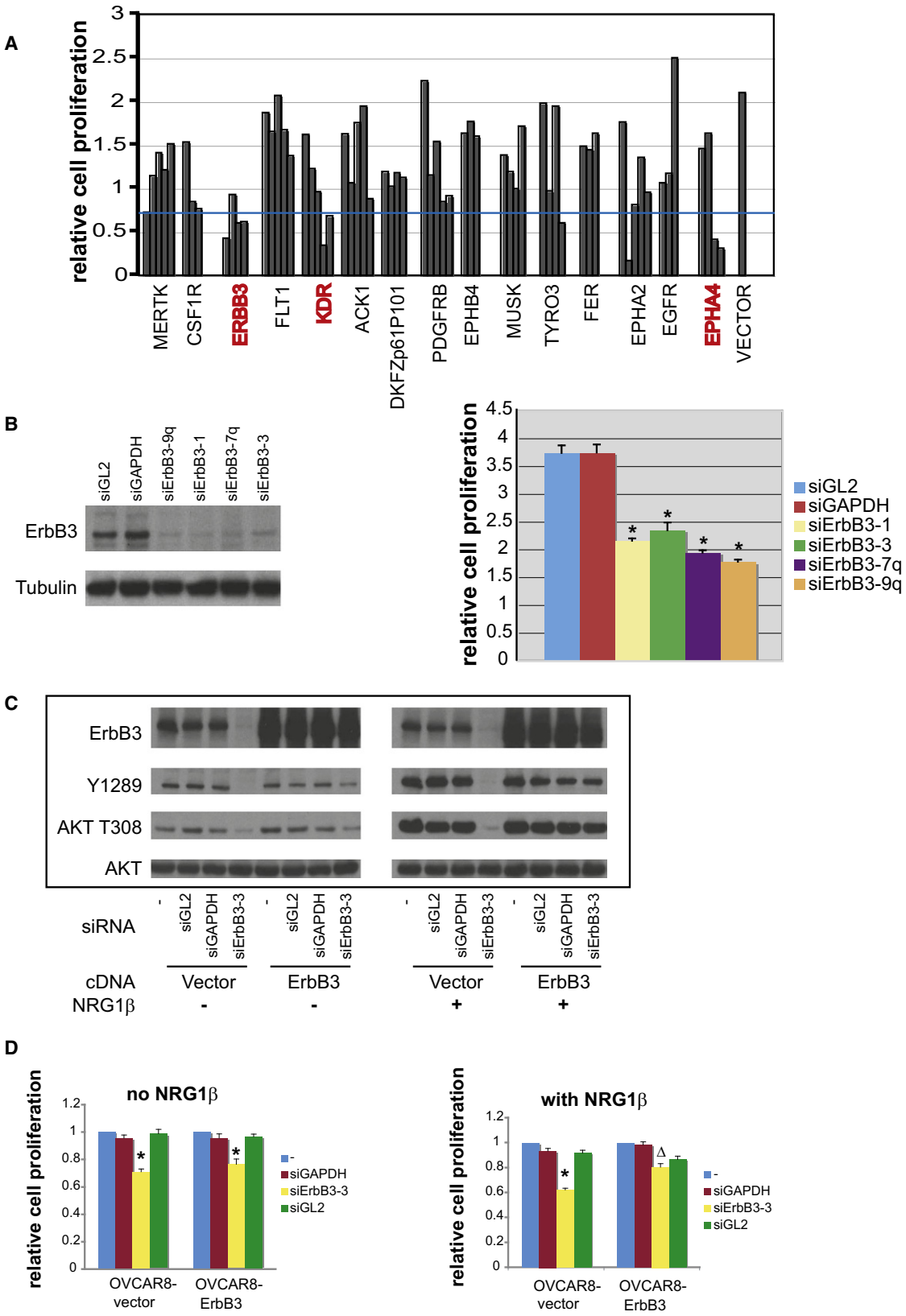

Figure 1. Depletion of ErbB3 Inhibits OVCAR8 Proliferation

(A) Secondary shRNA kinase screen in which 15 hairpin sets, each of which scored at least one hit in the primary screen, were retested. Each bar represents the effect of one hairpin; shRNAs directed against the same kinase are grouped together. Hairpin sets containing ≥2 hits in the secondary screen were considered

1994; Soltoff et al., 1994). To determine whether cell proliferation was perturbed when activated ErbB3 was depleted, we first compared the response to forced ErbB3 depletion of two ovarian cancer cell lines, OVCAR8 (which expresses and activates ErbB3) and OVCAR5 (which expresses ErbB3 protein but does not activate it). Three separate OVCAR5 and OVCAR8 sublines, each carrying a different nonoverlapping tet-inducible shErbB3, and a fourth subline carrying a tet-inducible "scrambled" shRNA were established. In the absence of doxycycline, the proliferation rate of all shRNA-carrying lines was comparable to that of control cell lines. However, upon doxycycline induction of shErbB3 expression, proliferation of all of the shErbB3 OVCAR8 sublines was substantially reduced (Figure 2B). In contrast, despite efficient reduction of ErbB3 protein levels in OVCAR5 cells, the same shErbB3 hairpins had only minimal or no effect on cell proliferation (Figure 2C). The difference in response between OVCAR8 and OVCAR5 cells to loss of ErbB3 suggests that cells which constitutively activate ErbB3 are also dependent upon the protein for cell proliferation, whereas those that produce but fail to activate it are not. In keeping with this notion, SKOV3, another ovarian cancer cell line that, like OVCAR8, expresses a high level of activated ErbB3, was sensitive to doxycycline-induced shErbB3 synthesis. In contrast, IGROV-1, an ovarian cancer cell line that resembles OVCAR5 with respect to ErbB3 expression and activation, was not (Figure 2D). The NRG1, ErbB3, and activated ErbB3 status, as well as the sensitivity to ErbB3 RNAi for a panel of ovarian cancer cell lines, is shown in Table S2. In five of the lines tested for shErbB3 sensitivity, the NRG1 and phospho-ErbB3 phenotypes predicted the outcome of depleting ErbB3, whereas in four cell lines with an NRG1/activated-ErbB3 phenotype, ErbB3 depletion did not result in cell toxicity, suggesting that additional signal transduction events may compromise a straightforward dependence upon ErbB3 or NRG1.

Existence of an NRG1/ ErbB3 Autocrine Loop in Ovarian Cancer Cells

Certain mechanisms that could, in principle, lead to sustained ErbB3 activation in OVCAR8 cells were evaluated. The entire coding sequence of *ERBB3* in 145 primary ovarian carcinoma DNA samples was sequenced, and no somatic *ERBB3* mutations were detected (data not shown). A missense mutation was identified in the *ERBB2* open reading frame (G776V) in OVCAR8 cells. However, shRNA-mediated depletion of neither EGFR nor Her-2 in OVCAR8 led to ErbB3 deactivation (data not shown). These cells do not synthesize detectable amounts of ErbB4 (data not shown). Because it had been reported previously that some ovarian cancer cells secrete the ErbB3 ligand NRG1 (Gilmour et al., 2002), we tested for the presence of an NRG1/ErbB3 autocrine loop in OVCAR8 and other lines that produce and activate ErbB3.

RT-PCR revealed the presence of NRG1 mRNA in OVCAR8 and SKOV3 cells, both of which contain activated ErbB3, but not in OVCAR5 or IGROV-1 cells, which express ErbB3 but do not constitutively activate it (Figure 3A, left). Immunoblotting of conditioned medium (CM) derived from OVCAR8 cultures using an antibody directed against NRG1 revealed an ~50 kD band (Figure 3A, middle). This band was absent from OVCAR5 CM (not shown). Transfer of CM from either OVCAR8 or SKOV3 to OVCAR5 induced activation of ErbB3 and AKT in the latter (Figure 3B). Moreover, two NRG1-directed siRNAs each resulted in a significant reduction in the abundance of the 50 kD band in OVCAR8 CM (Figure 3A, middle). Similarly, CM obtained from NRG1 siRNA-treated OVCAR8 cells was less effective in activating ErbB3 and AKT in OVCAR5 cells than CM from control siRNA-treated cells (Figure 3A, right). In addition, OVCAR8 cells treated with NRG1 siRNAs (1.4 and 1.9) revealed less ErbB3 activation than the control (Figure 3C, left), further supporting the hypothesis that NRG1 is an autocrine stimulator of ErbB3 activation in OVCAR8.

To investigate the role of NRG1 in cells bearing a putative NRG1/activated-ErbB3 autocrine phenotype, the effect of NRG1-directed RNAi on cell proliferation was tested. Multiple siRNAs directed against NRG1 resulted in OVCAR8 proliferation inhibition (Figure S3A). This effect was reversed by expression of an NRG1 cDNA that was immune to one of the two siRNAs depicted in Figure 3C (i.e., siNRG1.4). In contrast, no reversal was observed when cells expressing the siNRG1.4-immune NRG1 cDNA were transfected with a different NRG1-directed siRNA (siNRG1.9) to which the cDNA was not immune. As with tet-inducible shRNAs directed at ErbB3, doxycycline-mediated synthesis of two shRNAs directed at NRG1 resulted in significant toxicity in OVCAR8 and SKOV3 cells but only minimal toxicity in OVCAR5 and IGROV-1 cells, neither of which produce NRG1 mRNA (Figures S3B–S3D).

We also searched for evidence of an NRG1/ErbB3 autocrine loop in fresh primary tumor cells derived from malignant ascites fluid obtained from patients with advanced ovarian cancer. Of tumor cells derived from the 20 samples that were analyzed, 6 expressed comparatively high levels of NRG1 mRNA (Figure 4A). Three of these NRG1-expressing samples were subsequently tested further (DF14, DF25, DF26). Each contained activated ErbB3 that could be coimmunoprecipitated with the p85 subunit of PI3 kinase (Figure 4B), consistent with the hypothesis that,

positives in that screen and marked in red. The blue line denotes the point representing one standard deviation below the mean value of all CellTiter-Glo data obtained in this assay. See Table S1 for complete results of the screen.

(B) siRNA species directed against ErbB3 inhibited OVCAR8 proliferation. Left: ErbB3 protein level in OVCAR8 cells treated with either control siRNA or different siErbB3 species. Right: proliferation of OVCAR8 cells treated with either control siRNA or siErbB3. *significantly different from siGL2- or siGAPDH-treated sample ($p < 0.05$, Student's t test). See also Figure S1 for effects of shErbB3.

(C) Biochemical effects of overexpressing an ErbB3 cDNA immune to ErbB3 siRNA in the absence and presence of recombinant NRG1β (see Supplemental Experimental Procedures).

(D) Effect on OVCAR8 proliferation of overexpressing an ErbB3 cDNA immune to ErbB3 siRNA in the absence and presence of NRG1β. In the vector-only control cells, growth of ErbB3 siRNA cells was significantly different from siGL2- and siGAPDH-treated samples (*$p < 0.05$, Student's t test). In cells stably expressing siRNA-resistant ErbB3 cDNA in the presence of exogenous NRG-1β, growth of cells treated with ErbB3 siRNA was significantly greater than in the vector-only cells ($^{\Delta}p < 0.05$, Student's t test).

Error bars represent ± SD.

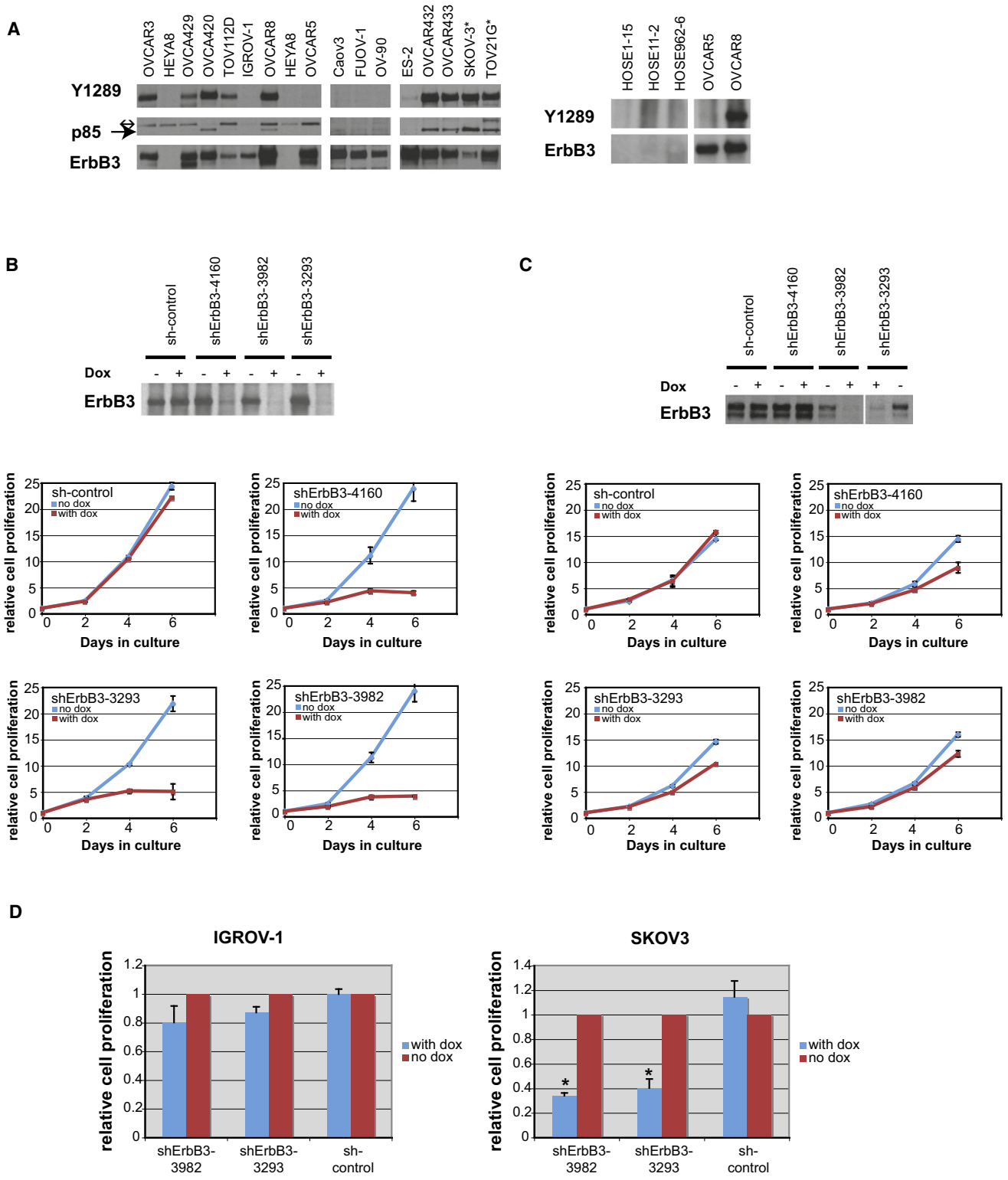

Figure 2. ErbB3 Is Activated in Multiple Ovarian Cancer Cell Lines

(A) Study of ErbB3 expression and activation in various ovarian cancer cell lines. Left: lysates were immunoprecipitated with anti-ErbB3 antibody and then blotted with anti-phospho-ErbB3 (Y1289) and anti-PI3K p85 antibody. The Y1289 blot was then stripped and reprobed with anti-ErbB3 antibody. *5 mg of lysate was applied for TOV21G and SKOV3 cells due to the relatively low abundance of ErbB3 in these cell lines. For all other cell lines, 1 mg of lysate was used. ↔, a background band; →, p85. Right: ErbB3 expression was not detected in normal ovarian surface epithelial cells. See also Figure S2 for EGFR and Her-2 status.

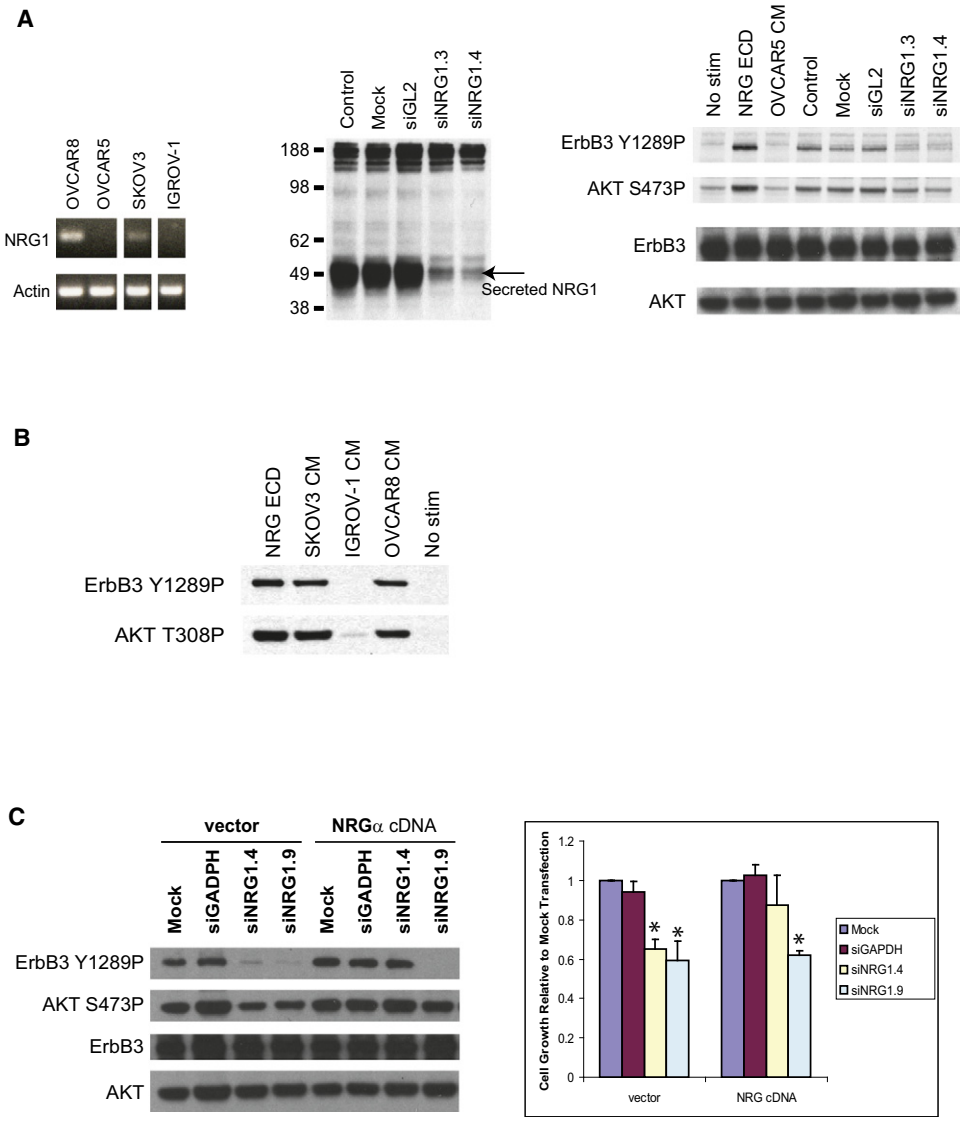

Figure 3. OVCAR8 ErbB3 Phosphorylation Is Mediated by NRG1 which, when Depleted, Results in Proliferation Inhibition

(A) Left: NRG1 mRNA is present in OVCAR8 and SKOV3 cells but not in OVCAR5 or IGROV-1 cells. Middle: NRG1-directed RNAi depleted the CM of OVCAR8 of the 50 kD anti-NRG1 reactive band as compared to mock or siGL2. Right: it also reduced the ability of OVCAR8 CM to mediate phosphorylation of ErbB3 in OVCAR5 cells.

(B) Transfer of CM from OVCAR8 or SKOV3 or recombinant NRG1 polypeptide mediated the phosphorylation of ErbB3 in OVCAR5.

(C) Expression of an NRG1 cDNA resistant to the NRG1-directed siRNA siNRG1.4 led to restoration of intrinsic ErbB3 phosphorylation in OVCAR8 and prevention of toxicity when the cells were treated with siNRG1.4; this did not occur in cells exposed to siNRG1.9, to which the cDNA is not immune. *significantly different from mock and siGAPDH samples ($p < 0.05$, Student's t test). Error bars represent ± SD. See Figure S3 for effect of NRG1 depletion on ovarian cancer cell lines.

in vivo, the PI3 kinase pathway had been engaged through NRG1-driven activation of ErbB3. In one of these primary cell preparations (DF14), ErbB3 coimmunoprecipitated with both Her-2 and ErbB4 (Figure 4C). In addition, CM from some of the primary tumor cell samples that express NRG1 mRNA (DF05, DF14) activated ErbB3 in OVCAR5 cells (which express but do

(B) Doxycycline-induced shErbB3 inhibits OVCAR8 cell proliferation. Top: ErbB3 protein level in OVCAR8 cells carrying three different doxycycline-inducible shErbB3 species or a doxycycline-inducible control shRNA in the presence or absence of doxycycline. Bottom: OVCAR8 proliferation in cells expressing different doxycycline-inducible shRNAs in the presence or absence of doxycycline.

(C) Top: OVCAR5 cell expression of ErbB3 before and after doxycycline-induced ErbB3 hairpin expression. Bottom: doxycycline-induced shErbB3 elicited only limited effects on OVCAR5 proliferation.

(D) Effect of inducible shErbB3 on IGROV-1 (left) and SKOV3 (right) cells. *significantly different from shControl sample ($p < 0.05$, Student's t test). Error bars represent ± SD. See Table S2 for a summary of additional ovarian cancer cell lines.

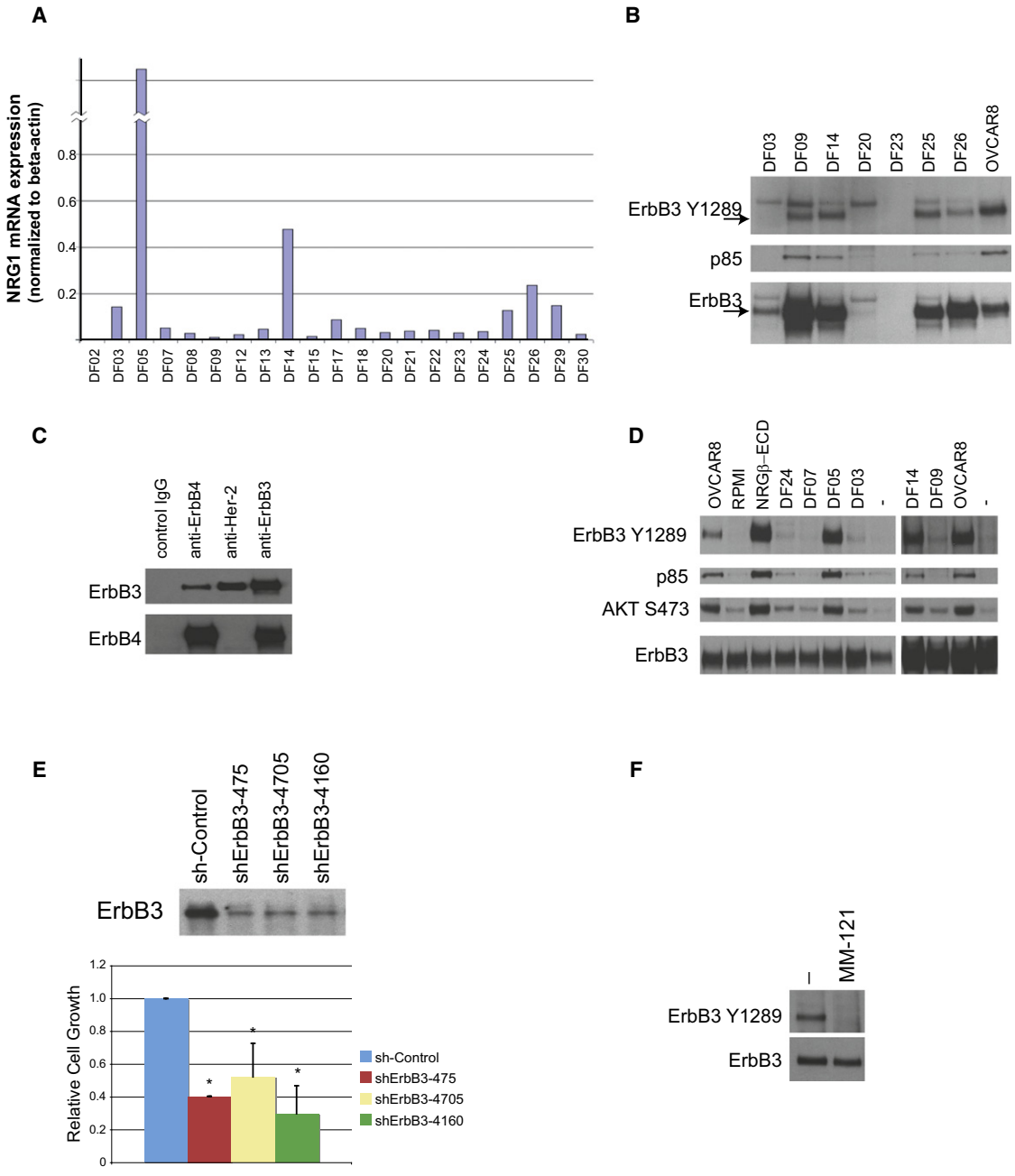

Figure 4. ErbB3 Is Expressed and Phosphorylated and NRG1 Is Expressed in a Subset of Primary Human Ovarian Cancers

(A) A subset of primary human ovarian cancer cells was analyzed for NRG1 mRNA, as detected by quantitative RT-PCR.

(B) ErbB3 is expressed and activated in a subset of primary human ovarian cancer cells. The p85 subunit of PI3K was coimmunoprecipitated in cells that phosphorylate ErbB3 on Y1289, consistent with active signaling through the PI3 kinase pathway.

(C) ErbB3 interacts with ErbB4 and Her-2 in primary DF14 ovarian cancer cells. DF14 lysates were immunoprecipitated with either control IgG or antibodies directed at either ErbB4, Her-2, or ErbB3, followed by immunoblotting with either anti-ErbB3 or anti-ErbB4.

(D) Conditioned medium from primary human ovarian cancer cells that intrinsically phosphorylate ErbB3 elicited ErbB3 phosphorylation and PI3K/AKT pathway activation following transfer to OVCAR5 cells.

(E) Top: ErbB3-directed shRNA effectively reduced ErbB3 protein expression levels in DF14 cells. Bottom: three different shErbB3s resulted in growth inhibition in DF14 cells. *significantly different from shControl ($p < 0.05$, Student's t test). Error bars represent ± SD.

(F) A monoclonal antibody directed against the ErbB3 ectodomain (MM-121) abolished endogenous DF14 ErbB3 phosphorylation.

not activate ErbB3) (Figure 4D). Depletion of ErbB3 by shRNA in a culture of one of the primary ovarian cancer cell strains that demonstrates this NRG1/activated-ErbB3 phenotype (DF14) resulted in decreased cell proliferation (Figure 4E), supporting the notion that ErbB3 can play an important role in supporting cell growth in primary ovarian cancers. Furthermore, incubation

of the same cells, namely DF14, with a monoclonal antibody directed at the ErbB3 ectodomain (MM-121) abrogated phosphorylation of ErbB3 in these cells (Figure 4F). Taken together, the above-noted data strongly suggest that ErbB3 is activated by an NRG1-driven autocrine circuit in certain ovarian cancer cell lines and in a significant fraction of primary advanced-stage ovarian cancers. As seen in Figure 4C, this activation may involve ErbB3 heterodimerization with a suitable kinase-competent ErbB family member (e.g., Her-2 or ErbB4).

Loss of ErbB3 Inhibits Growth in Three-Dimensional Culture and Decreases Tumor Progression in Mouse Xenograft Models

We also asked whether loss of ErbB3 inhibits growth of OVCAR8 cells in 3D culture, as represented in a spheroid formation assay. Using a hanging-droplet method, spheroids were created from OVCAR8 cells transduced with inducible ErbB3-directed or control shRNAs. Induction of the shErbB3s with doxycycline inhibited spheroid formation as compared with a scrambled shRNA derivative. This effect was particularly pronounced in the cell population that synthesized the 3293 shRNA (Figure 5A).

Given the cell-culture data suggesting that ErbB3 is indispensable for proliferation of human ovarian cancer cell lines that display evidence of an autocrine NRG1/activated-ErbB3 circuit, we also asked whether perturbation of this pathway affects tumor progression in an intraperitoneal OVCAR8 xenograft mouse model. Preinjection shRNA-mediated depletion of ErbB3 followed by continuous doxycycline treatment of mice that had been injected intraperitoneally with the pretreated cells significantly decreased tumor progression compared with controls, as measured by an increase in whole-animal luciferase activity detected by in vivo bioluminescent imaging (Figure 5B). Induction of two different ErbB3 hairpins by initiation of doxycycline treatment after tumor establishment (reflected by an increase in luciferase activity after intraperitoneal tumor cell injection) reduced tumor progression and significantly improved overall survival in both cases (Figures 5C and 5D). No suppression of tumor progression was detected following the induction of a scrambled shRNA (Figure S4A). Of note, these in vivo effects correlated with the results of the 3D culture seen in Figure 5A, with induction of 3293 shRNA resulting in more significant defects in spheroid formation and tumor regression in the mice xenografts than 3982 shRNA. The difference in effect between these two shRNA species may be explained by their differing potencies in inducing rapid ErbB3 depletion in vivo and in suspension culture (Figure S4B).

We also assessed the effects of an anti-ErbB3 ectodomain-directed monoclonal antibody, MM-121 (Merrimack Pharmaceuticals; previously described in Schoeberl et al., 2009), which, in biochemical assays, blocked both constitutive and NRG1-stimulated ErbB3 phosphorylation in OVCAR8 cells and elicited a small decrease in the OVCAR8 ErbB3 protein level (Figure S4C). In the ex vivo spheroid assay, MM-121 resulted in a small but consistent decrease in OVCAR8 spheroid growth (Figure 5E). In a subcutaneous xenograft model of OVCAR8 cells, significant inhibition of tumor growth was observed with MM-121 treatment compared with control-treated mice (Figure 5F). These observed antibody effects further underscore the importance of ErbB3 function for the maintenance of in vivo cell growth and suggest that the NRG1/ErbB3 circuit may be a viable therapeutic target in vivo.

DISCUSSION

A fraction of both established ovarian cancer cell lines and primary ovarian cancer-derived cell collections display a phenotype in which ErbB3, a member of the ErbB family of cell-surface receptor proteins, is activated. Activation of ErbB3 in a number of these ovarian cancer cells appears to be mediated by autocrine secretion of a known ErbB3 ligand, NRG1. In others, however, this activation may be NRG1 independent. The autocrine NRG1/ErbB3-activation effects contribute to a major biological outcome. When deprived of ErbB3 by RNAi, tumor cell lines that feature an active NRG1/ErbB3 circuit experienced a proliferation defect when grown on plastic surfaces, an effect that was overridden when the same cells were forced to overexpress a cognate RNAi-resistant ErbB3 cDNA in the presence of exogenous NRG1 ligand. These same tumor cell lines also demonstrated proliferation defects in the presence of NRG1 siRNA, and this effect could be overridden with the expression of an RNAi-resistant NRG1 cDNA. The proliferation defects observed with ErbB3 or NRG1 RNAi, thus, appear to be the product of on-target effects of the relevant RNAi reagents. In turn, these results indicate that this autocrine ErbB3-activating circuit supports one or more key steps in the mechanism underlying the ex vivo proliferation of the cell lines of interest.

Furthermore, when OVCAR8, which is tumorigenic after introduction into the peritoneal cavity of nude mice, was deprived of ErbB3 in culture through induced synthesis of a specific hairpin, de novo tumorigenesis was severely compromised. If the tumor cells were grown in doxycycline-free media and then exposed to the drug after the development of limited tumor growth in vivo, subsequent tumor growth was also blocked. Prolongation of the survival of the treated mice accompanied tumor growth blockade. Because exposure of these cells to a scrambled version of the ErbB3 hairpin led to no effect on tumor growth, an on-target effect of the relevant ErbB3 hairpins appears to be the basis for the in vivo tumor growth inhibition that was observed. The relevance of ErbB3 as a potential therapeutic target in ovarian cancer was supported by the ability of a systemically delivered, monoclonal anti-ErbB3 antibody to inhibit tumor growth in vivo in a xenograft model of OVCAR8 cells.

A role for activated ErbB3 in ovarian cancer proliferation was also suggested by analyses of primary ovarian cancer cells. A significant portion (4 of 7) of a collection of primary ovarian cancer cells freshly obtained from patients with advanced-stage disease revealed the presence of activated ErbB3 that coimmunoprecipitated with the p85 subunit of PI3 kinase (PI3K), sometimes together with expression of NRG1 mRNA. Given this evidence suggesting the presence of an NRG1/ErbB3 autocrine phenotype with associated biochemical engagement of the PI3K pathway in a subset of advanced-stage, primary, uncultured ovarian cancers, one suspects that this pathway could serve as a potential target in certain late-stage human ovarian cancers. This notion is supported by the evidence that ErbB3-directed RNAi inhibited cell growth of primary ovarian cancer cells that demonstrated evidence of an NRG1-producing/activated-ErbB3 phenotype (DF14) and that incubation of DF14 cells with

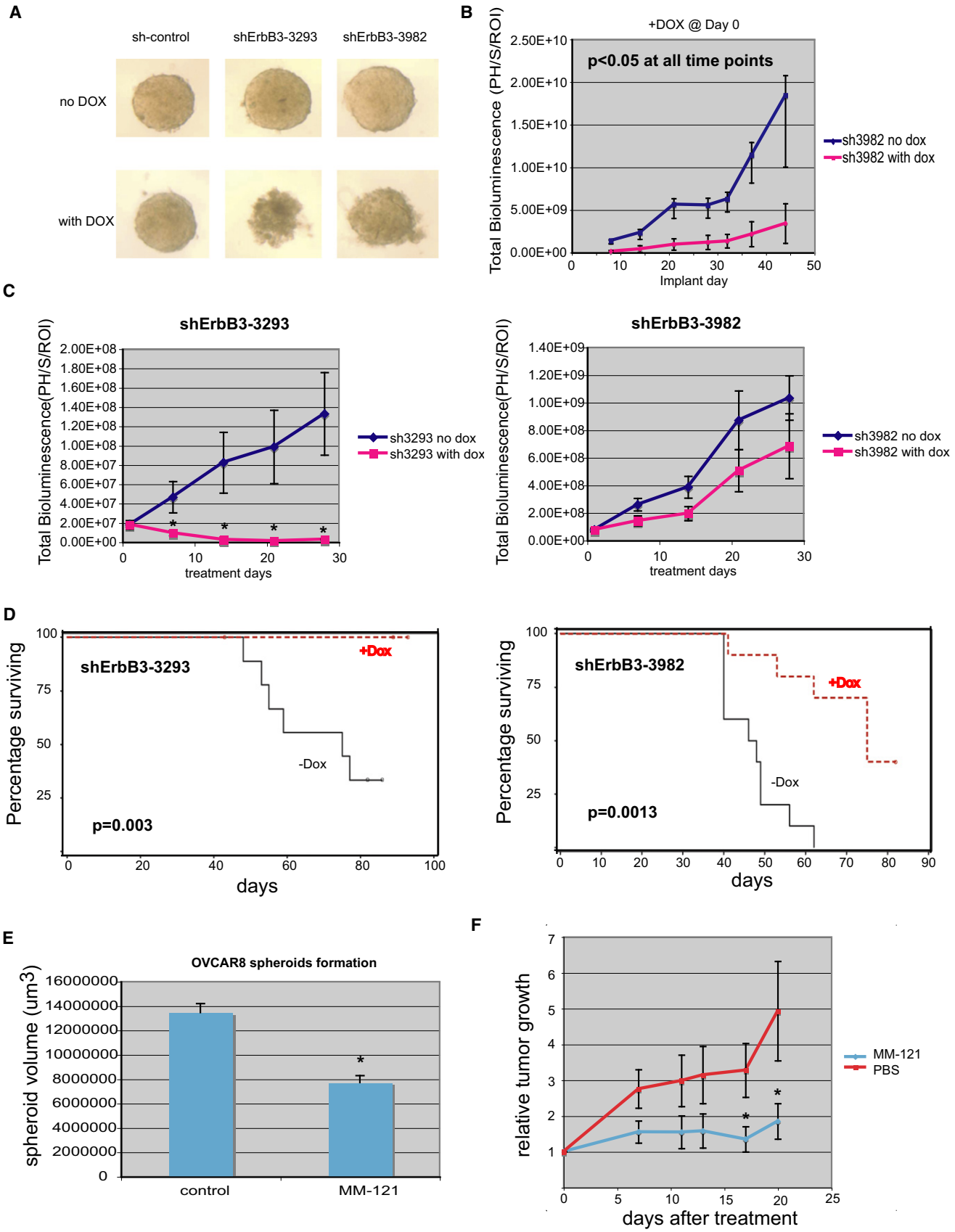
A
sh-control
shErbB3-3293
shErbB3-3982
no DOX
with DOX
B
+DOX @ Day 0
p<0.05 at all time points
Total Bioluminescence (PH/S/ROI)
Implant day
sh3982 no dox
sh3982 with dox
C
shErbB3-3293
Total Bioluminescence(PH/S/ROI)
treatment days
sh3293 no dox
sh3293 with dox
shErbB3-3982
sh3982 no dox
sh3982 with dox
D
shErbB3-3293
+Dox
-Dox
p=0.003
Percentage surviving
days
shErbB3-3982
p=0.0013
E
OVCAR8 spheroids formation
spheroid volume (um3)
control
MM-121
F
relative tumor growth
days after treatment
MM-121
PBS

a monoclonal ErbB3 antibody, MM-121, abolished endogenous Y1289 phosphorylation of ErbB3 in these cells. Thus, the phenomena described here are applicable to primary ovarian cancer cells in addition to established cell lines.

Of note, the effects of ErbB3 depletion were different when the same target cell line was grown on a plastic surface and when it was seeded as a peritoneal xenograft. In one case, ErbB3 depletion triggered proliferation arrest without clear signs of cell death. In contrast, in peritoneal xenografts, induction of the most potent ErbB3 shRNA resulted in tumor regression, suggesting that cell death had occurred. Whether this means that there is a dependency for viability on the NRG1/ErbB3 pathway when OVCAR8 tumor cells are cultivated as a three-dimensional tumor mass in vivo and a dependency for proliferation as opposed to viability when cultivated on a plastic surface is unclear.

Circumstantial evidence consistent with a role for ErbB3 in ovarian cancer is emerging (for reviews, see Lafky et al., 2008; Sithanandam and Anderson, 2008). ErbB3 and NRG1 expression have been observed in ovarian tumors, with a higher frequency in late-stage disease (Leng et al., 1997; Simpson et al., 1995a, 1995b), but the association of NRG1 expression and an activated ErbB3 circuit has not been previously observed. *ERBB3* gene amplification has been detected in some ovarian papillary-serous adenocarcinomas (Tsuda et al., 2004), and one study suggested that high ErbB3 expression is associated with reduced clinical survival (Tanner et al., 2006). Parenthetically, in neither OVCAR8 nor OVCAR5 is there evidence for *ERBB3* gene amplification, eliminating that phenomenon as the source of robust protein expression in these cells. Similarly, in neither OVCAR8 nor in the primary cell strain, DF14, both of which express NRG1, did we detect any evidence in single-nucleotide polymorphism array analyses for *NRG1* gene amplification, ruling out that possibility as the source of NRG1 expression in these lines (data not shown).

The therapeutic value of attacking ErbB3 in ovarian cancer patients remains unclear, and clinical trials with antibodies and small-molecule inhibitors directed at EGFR/Her-2, either of which can serve as an ErbB3 heterodimeric partner, have not demonstrated a significant benefit in ovarian cancer to date. In a phase II study, trastuzumab failed to demonstrate significant activity in ovarian cancers overexpressing Her-2, as assessed by immunohistochemistry (Bookman et al., 2003). Similarly, a phase II clinical trial with CI-1033, a pan-ErbB family inhibitor, demonstrated minimal activity in platinum-refractory patients (Campos et al., 2005). Moreover, pertuzumab, which inhibits Her-2 dimerization, particularly with ErbB3, failed to demonstrate significant benefit as a single agent in unscreened patients (Gordon et al., 2006). Notably, in a recent analysis of a randomized double-blind phase II trial comparing gemcitabine combined with placebo against gemcitabine combined with pertuzumab, patients with ErbB3 mRNA levels below the median observed in the study experienced significantly longer progression-free survival when treated with gemcitabine/pertuzumab compared with gemcitabine/placebo (Makhija et al., 2010). The mechanistic explanation for this remains unknown, and ErbB3 protein level and activation status were not examined in this study.

Despite the above-noted findings, the observation reported here of a functional NRG1/ErbB3 autocrine loop in a subset of ovarian cancer cells and cell lines and the potential importance of this pathway in maintaining ovarian cancer tumor growth suggests that this may be a population in which ErbB3-directed therapies should be considered. Given the observed interaction of ErbB3 with at least two ErbB family members, both of which are known to be enzymatically active, in both primary tumor cells (Figure 4C) and established cell lines (data not shown), combination treatment with agents that target ErbB3 and the relevant ErbB family members is also worth exploration.

ErbB3 can contribute to the function of Her-2 in sustaining cell transformation and tumor development (Holbro et al., 2003; Lee-Hoeflich et al., 2008). In breast cancer cells, resistance to toxicity from EGFR- or Her-2-directed small-molecule inhibitors could be mediated by restoration of ErbB3 phosphorylation, the mechanism of which may be due to increased ErbB3 localization to the cell surface (Sergina et al., 2007). Upon ErbB3 depletion, these cells again became sensitive to the effects of gefitinib (Sergina et al., 2007). Similarly, in an EGFR mutant-containing cell line that was initially sensitive to gefitinib, development of gefitinib resistance could be attributed to amplification of *MET*, which resulted in activation of ErbB3 through selective tyrosine phosphorylation. This, in turn, triggered unregulated AKT signaling (Engelman et al., 2007). These studies suggest that, in certain strains of *HER-2*-amplified breast cancer and mutant EGFR-producing lung cancer cells, activated ErbB3 plays a role in the development of resistance to inhibitors of Her-2 and EGFR kinase function. However, in principle, it might not be the primary driver of cancer cell proliferation and/or survival in these settings. In contrast, the data described here suggest that, in some ovarian cancer cells, ErbB3 is a primary stimulus to sustained cancer cell proliferation both in vitro and in vivo.

ErbB3, although a key member of the pathway(s) that triggers cultured cell proliferation and subsequent tumor development, is not sufficient to mediate these processes in isolation. The protein, even when overexpressed, must be activated to transduce relevant neoplastic growth signals. Two lines of evidence

Figure 5. Effect of ErbB3 Depletion on OVCAR8 Spheroid Formation and Tumor Progression

(A) Induction of shErbB3 inhibited OVCAR8 spheroid formation.

(B) Effect on tumor progression of inducing shErbB3 synthesis before inoculation of OVCAR8 cells into nude mice, with continued doxycycline treatment after injection. Error bars represent ± SEM. See Figure S4A for effect of shControl.

(C) Effect on tumor progression of inducing shErbB3 synthesis in OVCAR8 cells after tumor establishment. Error bars represent ±SEM.

(D) Kaplan-Meier survival plots of mice carrying two different tet-inducible shErbB3s. Mice were either treated with doxycycline or not, as indicated. See Figure S4B for an analysis of the relative potencies of sh3293 and sh3982.

(E) Monoclonal anti-ErbB3 antibody (MM-121) inhibited OVCAR8 spheroid growth. *significantly different from control sample ($p < 0.05$, Student's t test). Error bars represent ± SD.

(F) Monoclonal anti-ErbB3 antibody (MM-121) significantly inhibited OVCAR8 tumor growth in vivo in a xenograft model. Error bars represent ± SEM. See Figure S4C for biochemical effect of MM-121 in OVCAR8 cells.

support this claim. First, NRG1 depletion elicited proliferation arrest of OVCAR8 and SKOV3 cells, both NRG1-producing/activated-ErbB3-containing lines. Second, OVCAR5 cells, a line of ovarian cancer cells characterized by relatively high levels of ErbB3 but no NRG1 expression, do not demonstrate ErbB3 activation; these cells, in turn, are not sensitive to either ErbB3 or NRG1 depletion. In addition, NRG1 exposure triggered a marked increase in AKT phosphorylation/activation, presumably through a PI3K activation step. Thus, it seems reasonable to hypothesize that NRG1 synthesis and its binding to the ErbB3 ligand-binding domain or the existence of some other source of ErbB3 activation is required to elicit neoplastic effects in some ErbB3-producing ovarian cancer cells. In keeping with this hypothesis, others have failed to detect *ERBB3* mutations in 96 primary human ovarian cancers, suggesting that somatic *ERBB3* mutation is not a prominent pathway leading to its ovarian cancer-associated activation (R.K.T. and M.M., unpublished data).

Other tyrosine kinases can activate ErbB3. In mammary cancer cells, c-Src was shown to bind to ErbB3, and a c-Src family kinase inhibitor reduced ErbB3 phosphorylation (Contessa et al., 2006; Ishizawar et al., 2007; Zhang et al., 2007). More recently, as mentioned above, Engelman et al. reported that *MET* amplification leads to ErbB3 activation in the presence of an EGFR inhibitor (Engelman et al., 2007) and further demonstrated the presence of a MET/ErbB3/PI3K complex in these cells. Of note, we sought and failed to detect either MET activation or dependence on MET for the viability or proliferation of the ovarian cancer cells we tested. Conceivably, these are present in other primary ovarian cancer cell collections. Furthermore, in their paper, Sergina et al. demonstrated that AKT elicits a negative regulatory effect on ErbB3 phosphorylation, because PI3K inhibitors upregulated ErbB3 phosphorylation in mammary cancer cells that had been chronically exposed to an EGFR inhibitor(s) (Sergina et al., 2007). These data suggest the existence of a complex picture of the roles of certain ErbB family members, and of ErbB3 in particular, in cancer development and maintenance.

Finally, it is currently unclear when in the development of ovarian cancer ErbB3 activation takes place and whether, when such cells are first detected during tumor development, they represent all or only a fraction of available tumor cells. This notwithstanding, the findings cited here imply that the NRG1/ErbB3 circuit is active in primary ovarian cancer cells freshly obtained from certain advanced-stage patients. They also suggest that ErbB3- and/or NRG1-directed therapy is worth further experimental evaluation as potential treatment in the subset of human ovarian cancers in which there is an NRG1/ErbB3 autocrine growth-promoting phenotype. Phase I clinical trials are currently ongoing with ErbB3-directed monoclonal antibodies, and further exploration of the clinical efficacy of these or any other anti-ErbB3 agents currently in development in ErbB3-activated ovarian cancer is of interest.

EXPERIMENTAL PROCEDURES

Tyrosine Kinase shRNA Screen and Validation

See Supplemental Experimental Procedures for details.

Reagents and Antibodies

Antibodies directed at pErbB3 (Y1289), pAKT (T308), pAKT (S473), pMAPK (T202/T204), total MAPK, and total AKT were obtained from Cell Signaling Technology. Anti-ErbB3 C-terminal region Ab (clone 2F12) was from Lab Vision. Mouse monoclonal anti-PI3K p85 was from Upstate Biotechnology. Anti-NRG1-β-1 ECD monoclonal antibody (clone 147705) and recombinant human NRG1-β-1 ECD were from R&D Systems.

Plasmids and Cell Lines

Human ErbB3 cDNA (a gift from Dr. Lewis Cantley) was subcloned in the XhoI and NotI sites of pOZ-FH-C (Nakatani and Ogryzko, 2003). The primer sequences for subcloning ErbB3 cDNA were: 5′-gttaacgtcgacatggatagggc gaacgacgctctg-3′ and 5′-gttaacagcggccgcttacgttctctgggcattagcc-3′. An ErbB3 siRNA-resistant ErbB3 cDNA clone was generated with a QuikChange XL Site-Directed Mutagenesis Kit (Stratagene) using the primers 5′-cccgggtta gaggaggaagacgtaaatggctatgtcatgccagatac-3′ and 5′-gtatctggcatgacatagcc atttacgtcttcctcctctaacccggg-3′. Endogenous human NRG1 cDNA was cloned from OVCAR8 cells using the primer sequences 5′-tggaggcggccgcttatacagca atagggtcttgg-3′ and 5′-gttaacgcggccgctgaaccatggccgagcgcaaagaaggcag-3′ and subcloned into pBabe-hygro (Morgenstern and Land, 1990). NRG1 siRNA-resistant NRG1 cDNA clones were generated with a QuikChange XL Site-Directed Mutagenesis Kit using the primers 5′-gaatactcctctctcaggttt aaatggtttaaaaatgggaatgaattg-3′ and 5′-caattcattcccatttttaaaccatttaaacctgag agaggagtattc-3′.

To generate OVCAR8 cells carrying an siRNA-resistant ErbB3 mutant allele, 293FT cells were transfected with 1 μg of pOZ-FH-C carrying an siRNA-resistant ErbB3 cDNA and an IL-2 cDNA together with packaging plasmids, in the presence of Lipofectamine2000 (Invitrogen). Culture supernatants containing this siRNA-resistant ErbB3 and IL-2-encoding retrovirus were harvested 48 hr after transfection. Polybrene (4 μg/ml) was added to all viral supernatants prior to infection of OVCAR8 cells. Forty-eight hours after infection, infected cells were purified on anti-IL2-receptor antibody (Upstate Biotechnology) -coated Dynabeads (Invitrogen), as previously described (Nakatani and Ogryzko, 2003). OVCAR8 cells expressing NRG1 cDNAs for experiments involving cognate NRG1 siRNAs were generated by transfection of 293FT cells with 1 μg of suitable pBabe-hygro-NRG1 DNA together with packaging plasmids in the presence of Lipofectamine2000. Culture supernatants containing the desired NRG1 cDNA retrovirus were used to infect OVCAR8 cells. Forty-eight hours after infection, cells were selected for hygromycin resistance.

OVCAR8 cells carrying doxycycline-inducible shErbB3 or control shRNA were generated as follows. Sense and antisense oligonucleotides for shErbB3, namely shErbB3-3982, shErbB3-3293, shErbB3-4160, shErbB3-475, and shControl (for oligo sequences, see below) were annealed, phosphorylated with T4 kinase, and inserted into the AgeI and EcoRI sites of a "tet-on" PLKO vector (described in Wee et al., 2008). The resulting plasmids were then packaged and used to infect OVCAR8 cells. Infected OVCAR8 cells were selected for puromycin resistance and then pooled for subsequent use.

SKOV3, OVCAR8, and OVCAR5 were purchased from the American Type Culture Collection. Human ovarian surface epithelial cells were provided courtesy of Dr. Sam Mok. The other lines reported here were available in our laboratories. All cell lines were cultured in RPMI 1640 (Invitrogen) supplemented with 10% fetal bovine serum, 1× Pen/Strep (Invitrogen), and 1× glutamine (Invitrogen). Primary cell strains were cultured in RPMI 1640 supplemented with 10% fetal bovine serum and 1× antibiotic-antimycotic (Invitrogen). Cells were incubated at 37°C in a 5% CO_2-containing atmosphere.

Primary Cells

Primary cells were obtained from patients with advanced ovarian cancer at Dana-Farber Cancer Institute (DFCI) who underwent paracentesis for malignant ascites or debulking surgery under protocols approved by the Dana-Farber/Harvard Cancer Center Institutional Review Board (DFHCC IRB) and the Partners Human Research Committee. Consent from patients was obtained as per IRB guidelines. Ascites fluid was processed and tumor cells were purified according to a previously described protocol (Clauss et al., 2010). The epithelial nature of the cells for the cell packs was confirmed by EpCAM and HE4 antibody immunostaining. Only primary lines that were greater than 80% epithelial tumor cells after enrichment were selected for analysis. RNA was extracted using TRIzol. RNA- and protein-containing lysates were prepared from samples of fresh cells.

Cell Extracts, Western Blotting, and Immunoprecipitation

Modified SDS-free RIPA buffer (0.25% Na deoxycholate, 50 mM Tris-HCl [pH 7.4], 1% NP40, 150 mM NaCl, 1 mM EDTA) containing freshly added 50 mM NaF, 0.4 mM sodium orthovanadate, and complete protease inhibitor cocktail tablets (Roche) was used for extract preparation. For immunoprecipitation with mouse monoclonal Abs, lysates were incubated overnight with antibodies, anti-mouse immunoglobulin, and protein A beads at 4°C. Immunoprecipitates were washed three times with lysis buffer and resolved by SDS gel electrophoresis, and the separated proteins were blotted onto nitrocellulose membranes that were developed with appropriate antibodies.

RT-PCR

mRNA from cell lines was extracted with RNeasy Mini Kits (QIAGEN). Reverse transcription was performed with a SuperScript II First-Strand Synthesis Kit (Invitrogen). PCR and qRT-PCR were performed with SYBR-Green Supermix (Bio-Rad) with the following primers: actin (forward): 5′-ctggaacggtgaaggtg aca-3′; actin (reverse): 5′-aagggacttcctgtaacaatgca-3′; NRG1 (forward; exon 6): 5′-tcagtatccacagaaggagcaa-3′; and NRG1 (reverse; exon 7): 5′-atctcgag gggtttgaaagg-3′.

Spheroid Culture

Multicellular tumor spheroids were generated by the hanging-drop method (Kelm et al., 2003). A detailed description can be found in Supplemental Experimental Procedures. Where indicated, MM-121, a monoclonal anti-ErbB3 ectodomain antibody from Merrimack Pharmaceuticals, was added to a final concentration of 25 μg/ml on days 1 and 4 of spheroid formation.

Xenograft Studies

All xenograft studies were conducted under the guidelines of the DFCI Animal Research Facility with approved protocols. Inducible shErbB3 OVCAR8 cell lines were transduced with a luciferase-encoding allele as described (Rubin et al., 2003). OVCAR8 cells carrying different inducible shErbB3 hairpins were infected with pMMP-LucNeo-producing retrovirus (Rubin et al., 2003), and stable shRNA/luciferase-producing clones were selected in media containing 0.5 mg/ml G418 (Invitrogen). Xenografts were generated by injecting 1×10^6 cells intraperitoneally into 5- to 6-week-old NCr/nude mice (Taconic). Mice were anesthetized with a mixture of ketamine hydrochloride (150 mg/kg), xylazine (12 mg/kg), and D-luciferin (50 mg/ml) (Promega) and imaged using an In Vivo Imaging System (IVIS; Caliper Life Sciences) for a duration of 5–120 s per session. Mice recovered from anesthesia under isothermic conditions after imaging. To quantify bioluminescence, identical standardized circular regions of interest (ROI) were identified and positioned to encompass the areas of expected emission, and the integrated flux of photons through each ROI (photons/s) was quantitated using the Living Images software package (Caliper Life Sciences).

In a preinjection treatment tumor formation model, luciferase-producing OVCAR8 cells carrying a stably transfected tet-inducible ErbB3 hairpin (sh3982) were treated with 0.3 μg/ml doxycycline (Clontech) for 48 hr prior to mouse injection. Once injected, the recipient mice were continuously fed doxycycline-containing (2 mg/ml) or doxycycline-free water where indicated. Mice were then imaged weekly.

In a postinjection treatment model, luciferase-producing OVCAR8-sh3982 and a second, stably transfected, tet-inducible shErbB3-containing line, OVCAR8-sh3293, were grown in media lacking doxycycline and subsequently injected into mice. The animals were then imaged every 3–4 days until luciferase activity had increased during two serial measurements. These animals were then randomly separated into two groups. One was given water containing doxycycline, and the other group received doxycycline-free water. Subsequent imaging was performed weekly.

For the subcutaneous model, 1×10^7 OVCAR8 cells were mixed with Matrigel (BD Biosciences) at a 1:1 ratio and injected subcutaneously into irradiated nude mice. Once a measurable tumor appeared, MM-121 was injected intraperitoneally at 600 μg/mouse every 2 days. Control mice were injected with PBS. Tumor volumes were calculated with the formula $0.5^{*}T_{width}{}^{2*}T_{length}$.

siRNA and shRNA Sequences

See Supplemental Experimental Procedures for siRNA and shRNA sequences.

SUPPLEMENTAL INFORMATION

Supplemental Information includes four figures, two tables, and Supplemental Experimental Procedures and can be found with this article online at doi:10.1016/j.ccr.2009.12.047.

ACKNOWLEDGMENTS

We thank R. Wright and B. Ospina for expert technical assistance in mouse imaging. We would also like to thank Dr. S. Mok for providing human ovarian surface epithelial cells. This work was supported by NIH grants U54CA112962 (W.C.H.), W81XWH-07-0408 (W.C.H.), R33CA128625 (W.C.H.), and K12CA08772307 (J.F.L.); by NCI grants P50-CA105009 SPORE in Ovarian Cancer (Q.S., R.D.) and K08CA108748 (R.D.); by the DFCI/Novartis Program in Drug Discovery; by generous funding from the Women's Cancer Programs of DFCI; from the Ovarian Cancer Research Fund (R.D.); from the ASCO Young Investigator Award and Prevent Cancer Foundation (J.F.L.); from Deborah and Robert First (D.M.L., R.D.); the Joel and Randi Cutler Ovarian Research Fund (R.D.); and from the Aaron Foundation (D.M.L.). D.M.L., W.C.H., R.D., M.M., and A.L.K. are grantees of and consultants to the Novartis Institute of Biomedical Research. J.C., Z.M., D.B., and S.E. are employees and shareholders of the Novartis Institute of Biomedical Research. B.S. is an employee and shareholder of Merrimack Pharmaceuticals.

Received: March 17, 2009
Revised: December 2, 2009
Accepted: January 20, 2010
Published: March 15, 2010

REFERENCES

Apte, S.M., Bucana, C.D., Killion, J.J., Gershenson, D.M., and Fidler, I.J. (2004). Expression of platelet-derived growth factor and activated receptor in clinical specimens of epithelial ovarian cancer and ovarian carcinoma cell lines. Gynecol. Oncol. *93*, 78–86.

Blume-Jensen, P., and Hunter, T. (2001). Oncogenic kinase signalling. Nature *411*, 355–365.

Bookman, M.A., Darcy, K.M., Clarke-Pearson, D., Boothby, R.A., and Horowitz, I.R. (2003). Evaluation of monoclonal humanized anti-HER2 antibody, trastuzumab, in patients with recurrent or refractory ovarian or primary peritoneal carcinoma with overexpression of HER2: a phase II trial of the Gynecologic Oncology Group. J. Clin. Oncol. *21*, 283–290.

Campos, S., Hamid, O., Seiden, M.V., Oza, A., Plante, M., Potkul, R.K., Lenehan, P.F., Kaldjian, E.P., Varterasian, M.L., Jordan, C., et al. (2005). Multicenter, randomized phase II trial of oral CI-1033 for previously treated advanced ovarian cancer. J. Clin. Oncol. *23*, 5597–5604.

Clauss, A., Ng, V., Liu, J., Piao, H.-Y., Russo, M., Vena, N., Sheng, Q., Hirsch, M.S., Bonome, T., Matulonis, U., et al. (2010). Overexpression of elafin in ovarian carcinoma is driven by genomic gains and activation of the nuclear factor κB pathway and is associated with poor overall survival. Neoplasia *12*, 161–172.

Contessa, J.N., Abell, A., Mikkelsen, R.B., Valerie, K., and Schmidt-Ullrich, R.K. (2006). Compensatory ErbB3/c-Src signaling enhances carcinoma cell survival to ionizing radiation. Breast Cancer Res. Treat. *95*, 17–27.

Engelman, J.A., Zejnullahu, K., Mitsudomi, T., Song, Y., Hyland, C., Park, J.O., Lindeman, N., Gale, C.M., Zhao, X., Christensen, J., et al. (2007). MET amplification leads to gefitinib resistance in lung cancer by activating ERBB3 signaling. Science *316*, 1039–1043.

Gilmour, L.M., Macleod, K.G., McCaig, A., Sewell, J.M., Gullick, W.J., Smyth, J.F., and Langdon, S.P. (2002). Neuregulin expression, function, and signaling in human ovarian cancer cells. Clin. Cancer Res. *8*, 3933–3942.

Gordon, M.S., Matei, D., Aghajanian, C., Matulonis, U.A., Brewer, M., Fleming, G.F., Hainsworth, J.D., Garcia, A.A., Pegram, M.D., Schilder, R.J., et al. (2006). Clinical activity of pertuzumab (rhuMAb 2C4), a HER dimerization inhibitor, in advanced ovarian cancer: potential predictive relationship with tumor HER2 activation status. J. Clin. Oncol. *24*, 4324–4332.

Henriksen, R., Funa, K., Wilander, E., Backstrom, T., Ridderheim, M., and Oberg, K. (1993). Expression and prognostic significance of platelet-derived growth factor and its receptors in epithelial ovarian neoplasms. Cancer Res. *53*, 4550–4554.

Holbro, T., Beerli, R.R., Maurer, F., Koziczak, M., Barbas, C.F., III, and Hynes, N.E. (2003). The ErbB2/ErbB3 heterodimer functions as an oncogenic unit: ErbB2 requires ErbB3 to drive breast tumor cell proliferation. Proc. Natl. Acad. Sci. USA *100*, 8933–8938.

Hunter, T. (1998). The role of tyrosine phosphorylation in cell growth and disease. Harvey Lect. *94*, 81–119.

Ishizawar, R.C., Miyake, T., and Parsons, S.J. (2007). c-Src modulates ErbB2 and ErbB3 heterocomplex formation and function. Oncogene *26*, 3503–3510.

Jemal, A., Siegel, R., Ward, E., Hao, Y., Xu, J., and Thun, M. (2009). Cancer statistics, 2009. CA Cancer J. Clin. *59*, 225–249.

Kelm, J.M., Timmins, N.E., Brown, C.J., Fussenegger, M., and Nielsen, L.K. (2003). Method for generation of homogeneous multicellular tumor spheroids applicable to a wide variety of cell types. Biotechnol. Bioeng. *83*, 173–180.

Kim, H.H., Sierke, S.L., and Koland, J.G. (1994). Epidermal growth factor-dependent association of phosphatidylinositol 3-kinase with the erbB3 gene product. J. Biol. Chem. *269*, 24747–24755.

Lafky, J.M., Wilken, J.A., Baron, A.T., and Maihle, N.J. (2008). Clinical implications of the ErbB/epidermal growth factor (EGF) receptor family and its ligands in ovarian cancer. Biochim. Biophys. Acta *1785*, 232–265.

Lee-Hoeflich, S.T., Crocker, L., Yao, E., Pham, T., Munroe, X., Hoeflich, K.P., Sliwkowski, M.X., and Stern, H.M. (2008). A central role for HER3 in HER2-amplified breast cancer: implications for targeted therapy. Cancer Res. *68*, 5878–5887.

Leng, J., Lang, J., Shen, K., and Guo, L. (1997). Overexpression of p53, EGFR, c-erbB2 and c-erbB3 in endometrioid carcinoma of the ovary. Chin. Med. Sci. J. *12*, 67–70.

Makhija, S., Amler, L.C., Glenn, D., Ueland, F.R., Gold, M.A., Dizon, D.S., Paton, V., Lin, C.Y., Januario, T., Ng, K., et al. (2010). Clinical activity of gemcitabine plus pertuzumab in platinum-resistant ovarian cancer, fallopian tube cancer, or primary peritoneal cancer. J. Clin. Oncol., in press. Published online February 1, 2010.

Modesitt, S.C., and Jazaeri, A.A. (2007). Recurrent epithelial ovarian cancer: pharmacotherapy and novel therapeutics. Expert Opin. Pharmacother. *8*, 2293–2305.

Moffat, J., Grueneberg, D.A., Yang, X., Kim, S.Y., Kloepfer, A.M., Hinkle, G., Piqani, B., Eisenhaure, T.M., Luo, B., Grenier, J.K., et al. (2006). A lentiviral RNAi library for human and mouse genes applied to an arrayed viral high-content screen. Cell *124*, 1283–1298.

Morgenstern, J.P., and Land, H. (1990). A series of mammalian expression vectors and characterisation of their expression of a reporter gene in stably and transiently transfected cells. Nucleic Acids Res. *18*, 1068.

Mustelin, T., and Hunter, T. (2002). Meeting at mitosis: cell cycle-specific regulation of c-Src by RPTPα. Sci. STKE *2002*, pe3.

Nakatani, Y., and Ogryzko, V. (2003). Immunoaffinity purification of mammalian protein complexes. Methods Enzymol. *370*, 430–444.

Psyrri, A., Kassar, M., Yu, Z., Bamias, A., Weinberger, P.M., Markakis, S., Kowalski, D., Camp, R.L., Rimm, D.L., and Dimopoulos, M.A. (2005). Effect of epidermal growth factor receptor expression level on survival in patients with epithelial ovarian cancer. Clin. Cancer Res. *11*, 8637–8643.

Rubin, J.B., Kung, A.L., Klein, R.S., Chan, J.A., Sun, Y., Schmidt, K., Kieran, M.W., Luster, A.D., and Segal, R.A. (2003). A small-molecule antagonist of CXCR4 inhibits intracranial growth of primary brain tumors. Proc. Natl. Acad. Sci. USA *100*, 13513–13518.

Schoeberl, B., Pace, E.A., Fitzgerald, J.B., Harms, B.D., Xu, L., Nie, L., Linggi, B., Kalra, A., Paragas, V., Bukhalid, R., et al. (2009). Therapeutically targeting ErbB3: a key node in ligand-induced activation of the ErbB receptor-PI3K axis. Sci. Signal. *2*, ra31.

Seiden, M.V., Burris, H.A., Matulonis, U., Hall, J.B., Armstrong, D.K., Speyer, J., Weber, J.D., and Muggia, F. (2007). A phase II trial of EMD72000 (matuzumab), a humanized anti-EGFR monoclonal antibody, in patients with platinum-resistant ovarian and primary peritoneal malignancies. Gynecol. Oncol. *104*, 727–731.

Sergina, N.V., Rausch, M., Wang, D., Blair, J., Hann, B., Shokat, K.M., and Moasser, M.M. (2007). Escape from HER-family tyrosine kinase inhibitor therapy by the kinase-inactive HER3. Nature *445*, 437–441.

Sharma, S.V., and Settleman, J. (2007). Oncogene addiction: setting the stage for molecularly targeted cancer therapy. Genes Dev. *21*, 3214–3231.

Shepard, H.M., Lewis, G.D., Sarup, J.C., Fendly, B.M., Maneval, D., Mordenti, J., Figari, I., Kotts, C.E., Palladino, M.A., Jr., Ullrich, A., et al. (1991). Monoclonal antibody therapy of human cancer: taking the HER2 protooncogene to the clinic. J. Clin. Immunol. *11*, 117–127.

Simpson, B.J., Phillips, H.A., Lessells, A.M., Langdon, S.P., and Miller, W.R. (1995a). c-erbB growth-factor-receptor proteins in ovarian tumours. Int. J. Cancer *64*, 202–206.

Simpson, B.J., Weatherill, J., Miller, E.P., Lessells, A.M., Langdon, S.P., and Miller, W.R. (1995b). c-erbB-3 protein expression in ovarian tumours. Br. J. Cancer *71*, 758–762.

Sithanandam, G., and Anderson, L.M. (2008). The ERBB3 receptor in cancer and cancer gene therapy. Cancer Gene Ther. *15*, 413–448.

Soltoff, S.P., Carraway, K.L., III, Prigent, S.A., Gullick, W.G., and Cantley, L.C. (1994). ErbB3 is involved in activation of phosphatidylinositol 3-kinase by epidermal growth factor. Mol. Cell. Biol. *14*, 3550–3558.

Tanner, B., Hasenclever, D., Stern, K., Schormann, W., Bezler, M., Hermes, M., Brulport, M., Bauer, A., Schiffer, I.B., Gebhard, S., et al. (2006). ErbB-3 predicts survival in ovarian cancer. J. Clin. Oncol. *24*, 4317–4323.

Thaker, P.H., Deavers, M., Celestino, J., Thornton, A., Fletcher, M.S., Landen, C.N., Kinch, M.S., Kiener, P.A., and Sood, A.K. (2004). EphA2 expression is associated with aggressive features in ovarian carcinoma. Clin. Cancer Res. *10*, 5145–5150.

Tsuda, H., Birrer, M.J., Ito, Y.M., Ohashi, Y., Lin, M., Lee, C., Wong, W.H., Rao, P.H., Lau, C.C., Berkowitz, R.S., et al. (2004). Identification of DNA copy number changes in microdissected serous ovarian cancer tissue using a cDNA microarray platform. Cancer Genet. Cytogenet. *155*, 97–107.

Wee, S., Wiederschain, D., Maira, S.M., Loo, A., Miller, C., deBeaumont, R., Stegmeier, F., Yao, Y.M., and Lengauer, C. (2008). PTEN-deficient cancers depend on PIK3CB. Proc. Natl. Acad. Sci. USA *105*, 13057–13062.

Weinstein, I.B. (2002). Cancer. Addiction to oncogenes—the Achilles heal of cancer. Science *297*, 63–64.

Weinstein, I.B., and Joe, A.K. (2006). Mechanisms of disease: oncogene addiction—a rationale for molecular targeting in cancer therapy. Nat. Clin. Pract. Oncol. *3*, 448–457.

Weinstein, I.B., and Joe, A. (2008). Oncogene addiction. Cancer Res. *68*, 3077–3080.

Zhang, J., Kalyankrishna, S., Wislez, M., Thilaganathan, N., Saigal, B., Wei, W., Ma, L., Wistuba, I.I., Johnson, F.M., and Kurie, J.M. (2007). SRC-family kinases are activated in non-small cell lung cancer and promote the survival of epidermal growth factor receptor-dependent cell lines. Am. J. Pathol. *170*, 366–376.